ELSEVIER

Journal of Marine Systems 37 (2002) 87–105

JOURNAL OF MARINE SYSTEMS

www.elsevier.com/locate/jmarsys

Variability of the southern Antarctic Circumpolar Current front north of South Georgia

Sally E. Thorpe [a,b,*], Karen J. Heywood [a], Mark A. Brandon [b,1], David P. Stevens [c]

[a] School of Environmental Sciences, University of East Anglia, Norwich NR4 7TJ, UK
[b] British Antarctic Survey, Natural Environment Research Council, High Cross, Madingley Road, Cambridge CB3 0ET, UK
[c] School of Mathematics, University of East Anglia, Norwich NR4 7TJ, UK

Received 14 December 2000; received in revised form 15 November 2001; accepted 19 March 2002

Abstract

South Georgia (~ 54°S, 37°W) is an island in the eastern Scotia Sea, South Atlantic that lies in the path of the Antarctic Circumpolar Current (ACC). The southern ACC front (SACCF), one of three major fronts associated with the ACC, wraps anticyclonically around South Georgia and then retroflects north of the island. This paper investigates temporal variability in the position of the SACCF north of South Georgia that is likely to have an effect on the South Georgia ecosystem by contributing to the variability in local krill abundance.

A meridional hydrographic section that crossed the SACCF three times demonstrates that the SACCF is associated with a geopotential anomaly of 4.5 J kg^{-1} in the eastern Scotia Sea. A high resolution (1/4° × 1/4°) map of historical geopotential anomaly shows the mean position of the SACCF retroflection north of South Georgia to be at 36°W, 400 km further east than in previous work. It also reveals temporal variability associated with the SACCF in the South Georgia region. A near-surface drifter provides evidence for variability in the western extent of the SACCF north of South Georgia and for the presence of eddies in the region. Output from a 3-year (1993–1995) high frequency wind forced run of the eddy-permitting Ocean Circulation and Climate Advanced Modelling project (OCCAM) model, used to investigate the frontal variability, shows two periods of anomalous westward extent of the SACCF north of South Georgia and associated eddy-shedding. The SACCF variability affects the near-surface transport of passive drifters into the region with implications for the South Georgia ecosystem.

Keywords: Front; Temporal variability; Hydrographic data; Model; Dynamics; Krill; Southern Ocean; Scotia Sea [50–60°S, 45–30°W]

1. Introduction

South Georgia, an island in the eastern Scotia Sea [~ 54°S, 37°W; Fig. 1(a)], experiences dramatic interannual variability in its ecosystem. This variability is connected to fluctuations in the local abundance of Antarctic krill (*Euphausia superba*), the main food

* Corresponding author. Now at British Antarctic Survey, Natural Environment Research Council, High Cross, Madingley Road, Cambridge CB3 0ET, UK. Tel.: +44-1223-221400; fax: +44-1223-221259.
E-mail address: seth@bas.ac.uk (S.E. Thorpe).
[1] Now at Department of Earth Sciences, The Open University, Walton Hall, Milton Keynes MK7 6AA, UK.

0924-7963/02/$ - see front matter © 2002 Elsevier Science B.V. All rights reserved.
PII: S0924-7963(02)00197-5

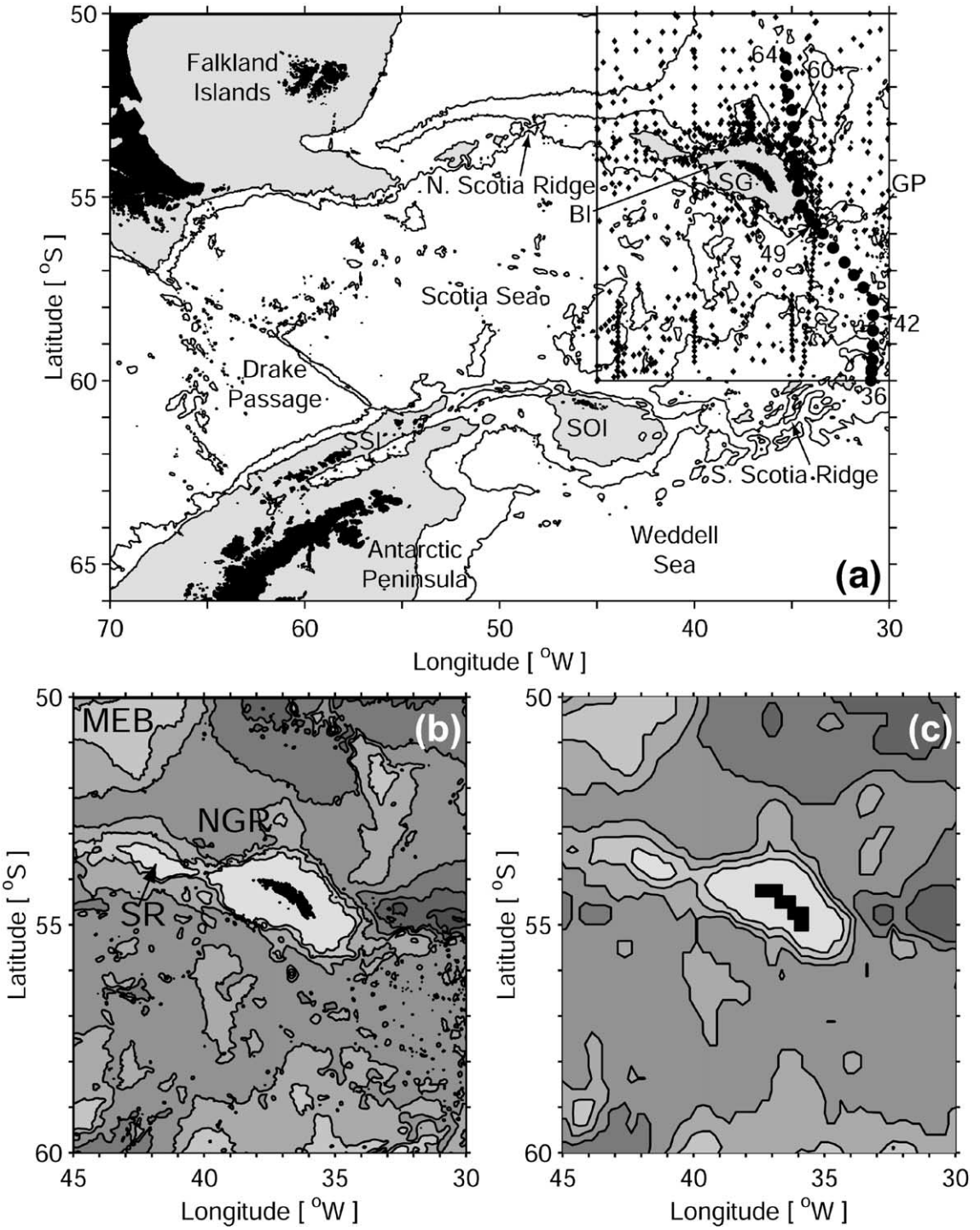
Falkland Islands
N. Scotia Ridge
Scotia Sea
Drake Passage
SI
SOI
S. Scotia Ridge
Antarctic Peninsula
Weddell Sea
(a)
64
60
SG
GP
BI
49
42
36
Latitude [°S]
Longitude [°W]
MEB
NGR
SR
(b)
(c)

source of the higher predators that breed on South Georgia (Croxall et al., 1988, 1999; Boyd et al., 1994). The krill population at South Georgia is believed not to be self-sustaining (Everson, 1984) but to be maintained instead by oceanic transport of krill from recognised breeding grounds upstream of South Georgia in the vicinity of the Antarctic Peninsula, the South Orkney Islands and the Weddell Sea (e.g. Everson, 1977; Murphy et al., 1998) [Fig. 1(a)]. Variability in krill abundance at one of these krill breeding grounds [the South Shetland Islands; Fig. 1(a)] has been linked to recruitment failure of different year classes (Siegel and Loeb, 1995). It has been proposed that this variability is related to sea-ice extent and duration (Marr, 1962; Loeb et al., 1997; Siegel et al., 1998). Research at Bird Island, just west of South Georgia [Fig. 1(a)], suggests that years of low krill abundance in the South Georgia region can be related to failure the previous year to recruit juvenile krill into the South Georgia population (Reid et al., 1999a,b). Given that the South Georgia krill population is thought to originate to some extent from the Antarctic Peninsula, propagation of the variability at the South Shetland Islands noted by Siegel and Loeb (1995) across the Scotia Sea might be expected. However, the variability in krill abundance observed at South Georgia cannot be entirely accounted for by the krill variability at the Antarctic Peninsula. Some year classes that are considered strong in the Antarctic Peninsula region can be completely absent from the South Georgia area (Murphy et al., 1998), raising the possibility of additional sources of variability operating in the South Georgia–Scotia Sea ecosystem. One such source is variability in the oceanic circulation affecting the transport of krill into the region. This paper addresses this issue using ocean general circulation model output, focussing on the region north of South Georgia.

The Scotia Sea is a relatively small basin in the southwestern Atlantic sector of the Southern Ocean. It is bounded by rugged bathymetry to the north, south and east (by the North Scotia Ridge, South Scotia Ridge and the South Sandwich Island Arc, respectively), and is open to Drake Passage to the west [Fig. 1(a)]. The central basin is generally deeper than 3000 m with relatively few topographic features whereas the eastern basin has more complex bathymetry. South Georgia lies at the eastern end of the North Scotia Ridge; to its east is a deep passage [Georgia Passage; Fig. 1(a)] that permits exchange between the Scotia Basin and the Georgia Basin to its north.

The Scotia Sea is influenced by two oceanographic regimes: the generally eastward flowing Antarctic Circumpolar Current (ACC) and the cyclonic circulation of the Weddell Gyre. Separating these is the Weddell–Scotia Confluence (Gordon, 1967), a mixture of the waters from the ACC and Weddell Gyre with water from the shelf of the northwest Weddell Sea (Whitworth et al., 1994). The ACC is a band of large zonal transport that circulates uninhibited around Antarctica. It is steered by regional bathymetry; in the Scotia Sea, the South Scotia Ridge deflects the southern part of the ACC northwards towards South Georgia. Within the ACC are cores of higher velocity current associated with thermohaline fronts. The southern ACC front (SACCF) has been identified as one of three major fronts in the ACC by Orsi et al. (1995). Lying between the Polar Front and the southern boundary of the ACC (SB), the SACCF crosses the central Scotia Sea and wraps around South Georgia before retroflecting north of the island (Orsi et al., 1995). The SACCF, the SB and the waters between the two fronts flow very close to the western continental shelf of the Antarctic Peninsula. Modelling studies have shown the importance of these waters and the SACCF, in particular, for transport to South Georgia from the Antarctic Peninsula region (Hofmann et al., 1998; Murphy et al., 1998).

Fig. 1. (a) Location of the study region in the eastern Scotia Sea (50–60°S, 45–30°W). Areas shallower than 1000 m are shaded grey and the 3000 m isobath is marked in black. Circles mark the station positions of the subsection of WOCE section A23 with selected stations numbered; diamonds mark the position of stations used in the historical geopotential anomaly analysis. Abbreviations for topographic features are as follows: BI—Bird Island; SG—South Georgia; GP—Georgia Passage; SSI—South Shetland Islands; SOI—South Orkney Islands. (b) Detailed bathymetry of the study region from the Smith and Sandwell (1997) dataset. Isobaths from 1000 m to 7000 m in intervals of 1000 m are shaded in darkening shades of grey. Additional topographic features marked are as follows: MEB—Maurice Ewing Bank; SR—Shag Rocks; NGR—North Georgia Rise. (c) Same as b but for the OCCAM bathymetry.

Early studies of the hydrography of the South Georgia region from the Discovery Investigations suggested that South Georgia is influenced by ACC water and water from the Weddell Sea (Deacon, 1933). The Discovery Investigations also revealed interannual variability in the oceanic conditions around South Georgia with warm and cold years evident from temperature measurements (Harmer, 1931; Deacon, 1977). Russian investigations provided further evidence of these temperature fluctuations (Maslennikov and Solyankin, 1979). A conclusion was drawn that the area north of South Georgia is highly variable with some years having greater ACC influence (and thus being warmer) and others having greater contribution from the Weddell Sea (therefore colder). More recently, analysis of hydrographic surveys occupied to the northwest of South Georgia has related the observed oceanographic variability to variability in the location of the SACCF north of South Georgia (Trathan et al., 1997, 2000) with warmer waters observed when the SACCF is located further east.

The South Georgia shelf has its own, distinct water mass (South Georgia Shelf Water; Brandon et al., 2000). Between this water and the deeper oceanic waters, a shelf break front has been observed on the northeastern South Georgia shelf but not to the northwest (Brandon et al., 1999, 2000). These near-shore dynamics will be important for the South Georgia ecosystem in transporting and retaining material on the South Georgia shelf. However, this paper focuses on the SACCF to the north of South Georgia and its associated variability. A review of the South Georgia ecosystem is given by Atkinson et al. (2001).

The SACCF, as with the other ACC fronts, is identified by large horizontal density gradients through the water column. The northern limit of the front can be identified from horizontal changes in the properties of Upper Circumpolar Deep Water (UCDW), a type of the Circumpolar Deep Water that occupies most of the deep layers of the ACC. From analysis of historical hydrographic sections, Orsi et al. (1995) locate stations north of the SACCF by: potential temperature (θ) greater than 1.8 °C along the θ-maximum of the UCDW at depths greater than 500 m; salinity (S) of more than 34.73 along the S-maximum (S_{max}) at depths greater than 800 m; and oxygen content of less than 4.2 ml l^{-1} along the oxygen minimum at depths greater than 500 m. Stations that are south of the SACCF, on the other hand, are apparent from the characteristics of the θ-minimum (θ_{min}) layer above the UCDW with $\theta < 0$ °C at depths shallower than 150 m south of the front.

Estimates of the geostrophic velocity of the SACCF in the Scotia Sea are lacking. Elsewhere, maximum geostrophic velocities of the SACCF (referenced to the deepest common level between station pairs) range from 0.05 to 0.1 m s^{-1} at ~140°E (Rintoul and Bullister, 1999) to 0.21 m s^{-1} at 30°E (Park et al., 2001) with a baroclinic transport of 22 Sv at 140°E (1 Sv = 10^6 m^3 s^{-1}; Rintoul and Bullister, 1999). Rintoul and Sokolov (2001), in an analysis of six repeats of the hydrographic section examined by Rintoul and Bullister (1999), observe two branches of the SACCF with transports of 18 ± 3 and 11 ± 3 Sv (± 1 standard deviation). Orsi et al. (1995) use a historical hydrographic section to calculate a baroclinic transport of approximately 15 Sv for the SACCF in the central Scotia Sea (relative to 3000 m or the deepest common level, not specified). Often the SACCF is too close to the SB for the two to be resolved as separate features, in which case, an estimate of the velocity and transport of the combined fronts is computed. Sparrow et al. (1996) derive a maximum geostrophic velocity of 0.04–0.06 m s^{-1} and transport of 35 Sv from gridded historical data for the SACCF and SB together at 60°E. Further east, Heywood et al. (1999) report a maximum geostrophic velocity of 0.1 m s^{-1} and a much smaller transport of 10 Sv at 85°E for the combined features.

In this paper, we study hydrographic data and model output to investigate the position and temporal variability of the SACCF north of South Georgia [Fig. 1(b)]. We use geopotential anomaly, calculated from a historical dataset, to locate the mean position of the SACCF in the study region. Although Orsi et al. (1995) have defined the location of the SACCF in this region from historical hydrographic sections, the use of geopotential anomaly yields a more accurate result by allowing more stations to be included as they do not need to be part of a section. The characteristics of the SACCF in a numerical eddy-permitting ocean general circulation model are

described. Variability of the position of the retroflection of the SACCF north of South Georgia is examined in 3 years of high frequency wind forced model output and the implications of the frontal variability for the South Georgia ecosystem are discussed.

2. The SACCF in observations

2.1. Characteristics of the SACCF in the eastern Scotia Sea

Hydrographic data from a subsection of the World Ocean Circulation Experiment (WOCE) section A23 (Heywood and King, 1996), conducted from RRS *James Clark Ross*, are used to establish a consistent definition for the SACCF in geopotential anomaly in the study region. We use data from the meridional subsection across the eastern Scotia Sea [Fig. 1(a)] occupied between 8 and 14 April 1995. Temperature and salinity were recorded with a Neil Brown MkIIIb CTD profiler, accurate to 0.001 °C and 0.002, respectively.

The SACCF was crossed three times by A23 (between station pairs 49–50, 58–59 and 60–61). The presence of the SACCF is evident in the θ–S space of the stations [Fig. 2(a)]: stations north of the SACCF have a fresher ($S \approx 33.95$) and slightly colder ($\theta \approx 0.5$ °C) θ_{min} than stations south of the SACCF ($S \approx 34.27$, $\theta \approx 0.75$ °C). Note that this is opposite to the property indicators of Orsi et al. (1995), who found that the θ_{min} is colder south of the SACCF and less than 0 °C (at all of the A23 stations θ_{min}>0 °C).

The SACCF crossings are visible in the full depth property sections [Fig. 3(a–d)]. North of South Georgia the frontal locations as defined in θ–S space are coincident with the limit of the 1.8 °C isotherm. South of South Georgia, the UCDW is slightly warmer and the front corresponds to $\theta \geq 1.9$ °C. The salinity of the S_{max} at the frontal crossings is less than the indicators of Orsi et al. (1995) with S generally >34.71 north of the front rather than 34.73. Each crossing of the SACCF has an associated current core reaching to depths of greater than 2000 m [Fig. 3(d)]. Maximum geostrophic velocities (referenced to the deepest common level between station pairs) are 0.1 m s^{-1} in the eastward-flowing crossings and -0.075 m s^{-1} in the westward-flowing crossing. These values are comparable to the velocity calculated by Rintoul and Bullister (1999) at ~140°E. The crossings of the SACCF have an associated baroclinic component of transport of 16.5, 13 and 14 Sv from north to south, respectively. These concur with the 15 Sv calculated by Orsi et al. (1995) in the central Scotia Sea and are within the ranges reported by Rintoul and Sokolov (2001) for the two branches of the SACCF at ~140°E.

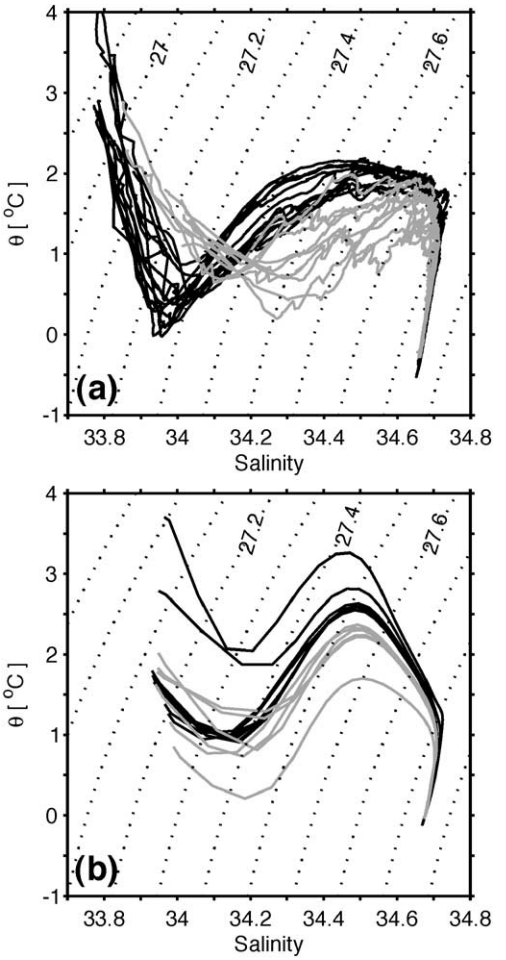

Fig. 2. θ–S profiles of the stations north of the SB along the WOCE A23 subsection. Stations north of the SACCF are black, stations south of the SACCF are grey. (a) A23 data; (b) OCCAM output. Isopycnals of σ_0 are marked.

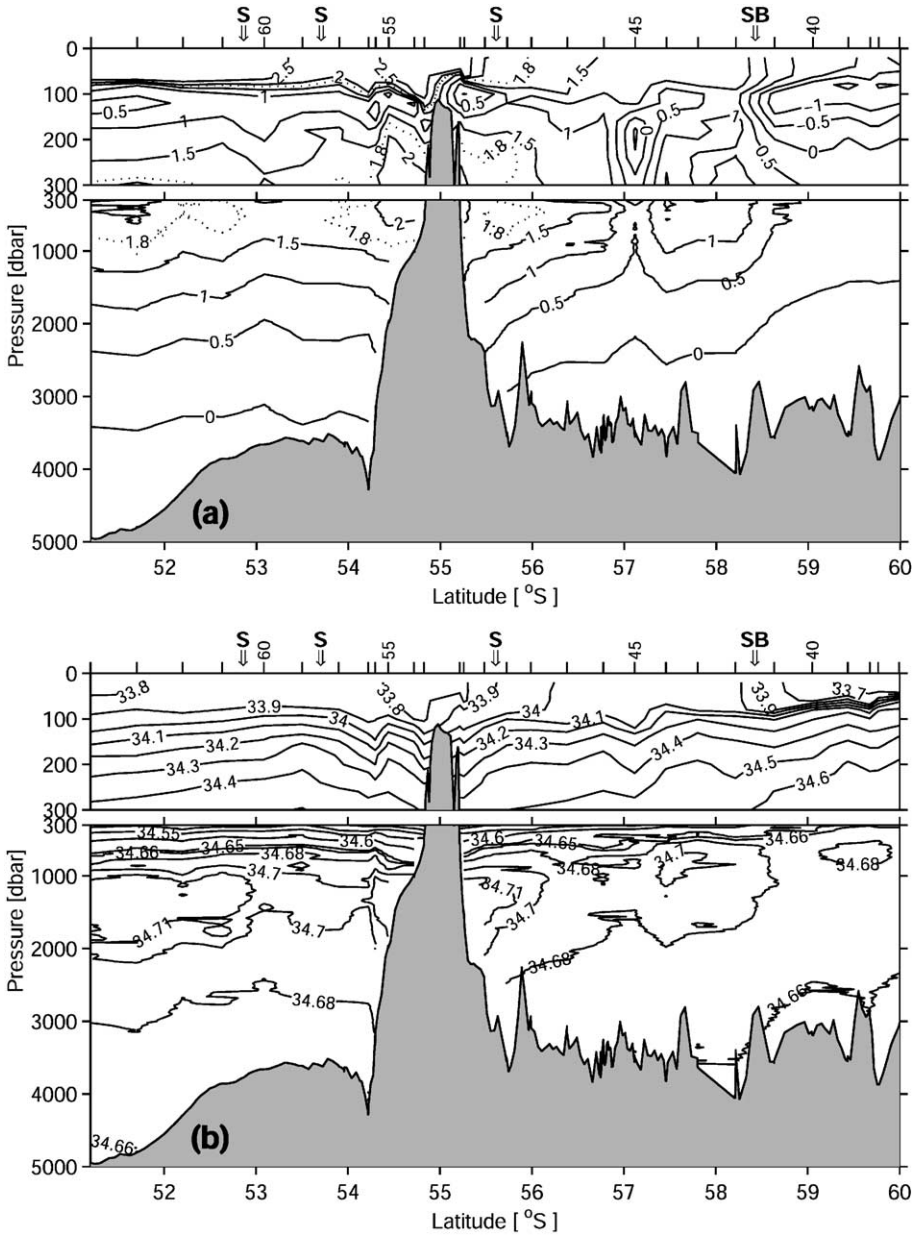

Fig. 3. Full depth property sections along the WOCE Section A23 subsection. Note that the upper 300 dbar of the water column is shown on an expanded vertical scale for clarity. (a) A23 potential temperature [°C], (b) A23 salinity, (c) A23 σ_0 for the upper 300 dbar, σ_2 below, (d) A23 geostrophic velocity referenced to the deepest common level between station pairs [m s^{-1}], westward flow is shaded grey. (e–h) The same as a–d but for the OCCAM output. Station positions are marked along the upper axis of each subplot. The position of each crossing of the SACCF is denoted with an S and the SB with SB.

Each crossing of the SACCF on A23, as determined from the θ–S characteristics, corresponds to a geopotential anomaly of 4.5 J kg^{-1} [50 dbar relative to 1000 dbar (these reference levels are discussed in the next section); Fig. 4]. Part of the A23 subsection (stations 35–52) was repeated 4 years later in 1999 as

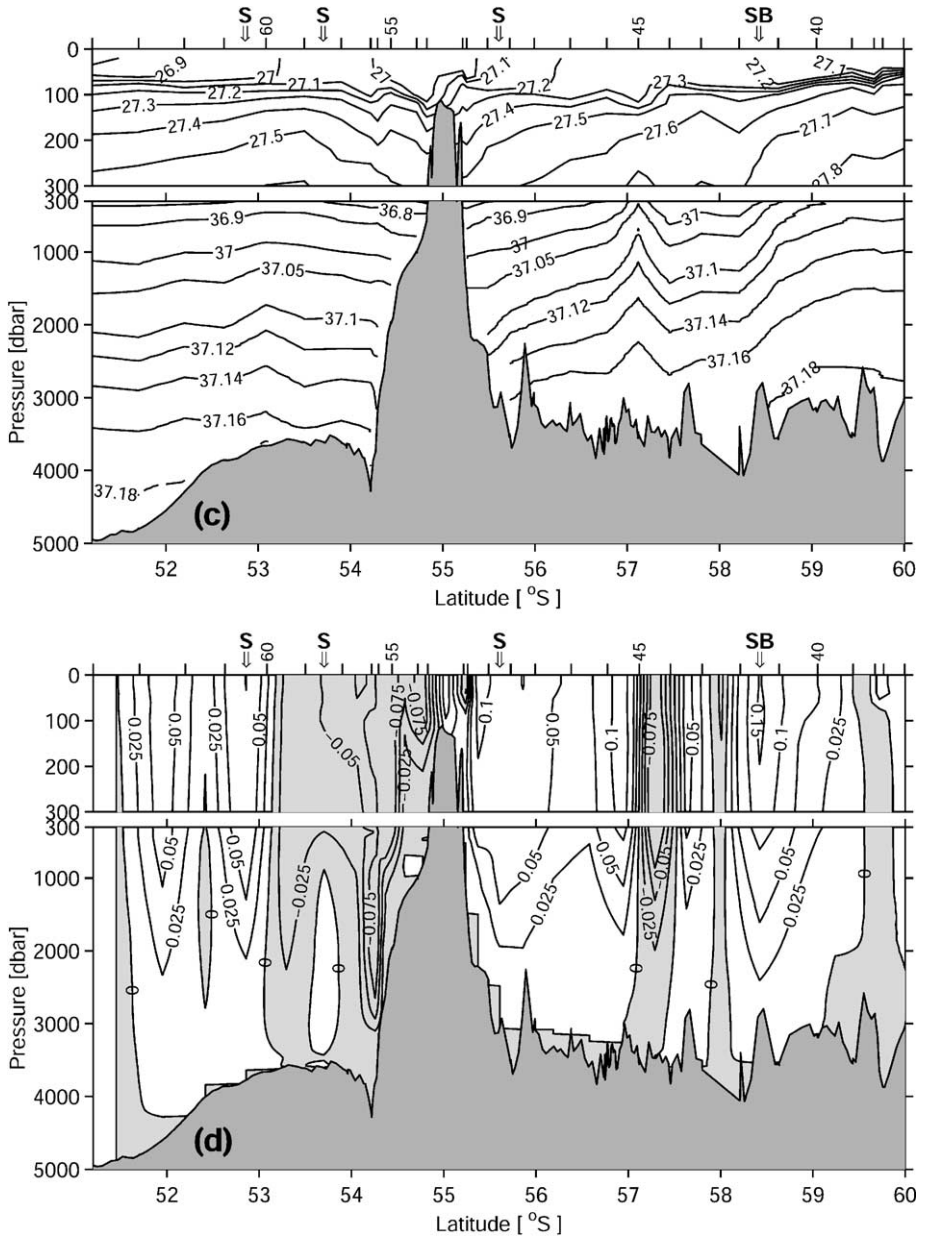

Fig. 3 (*continued*).

part of the Antarctic Large-Scale Box Analysis of the Role of the Scotia Sea (ALBATROSS) project (Meredith et al., 2001). The SACCF was crossed south of South Georgia (again near station 50) and as with the A23 data, the SACCF crossing corresponds to a geopotential anomaly of 4.5 J kg^{-1} (Thorpe, 2001). Interestingly, this value agrees with the geopotential anomaly quoted by Veth et al. (1997) for the SACCF in a section at 6°W. We now use this consistent geopotential anomaly characteristic of the SACCF to map the mean position of the SACCF in the vicinity of South Georgia using a historical dataset.

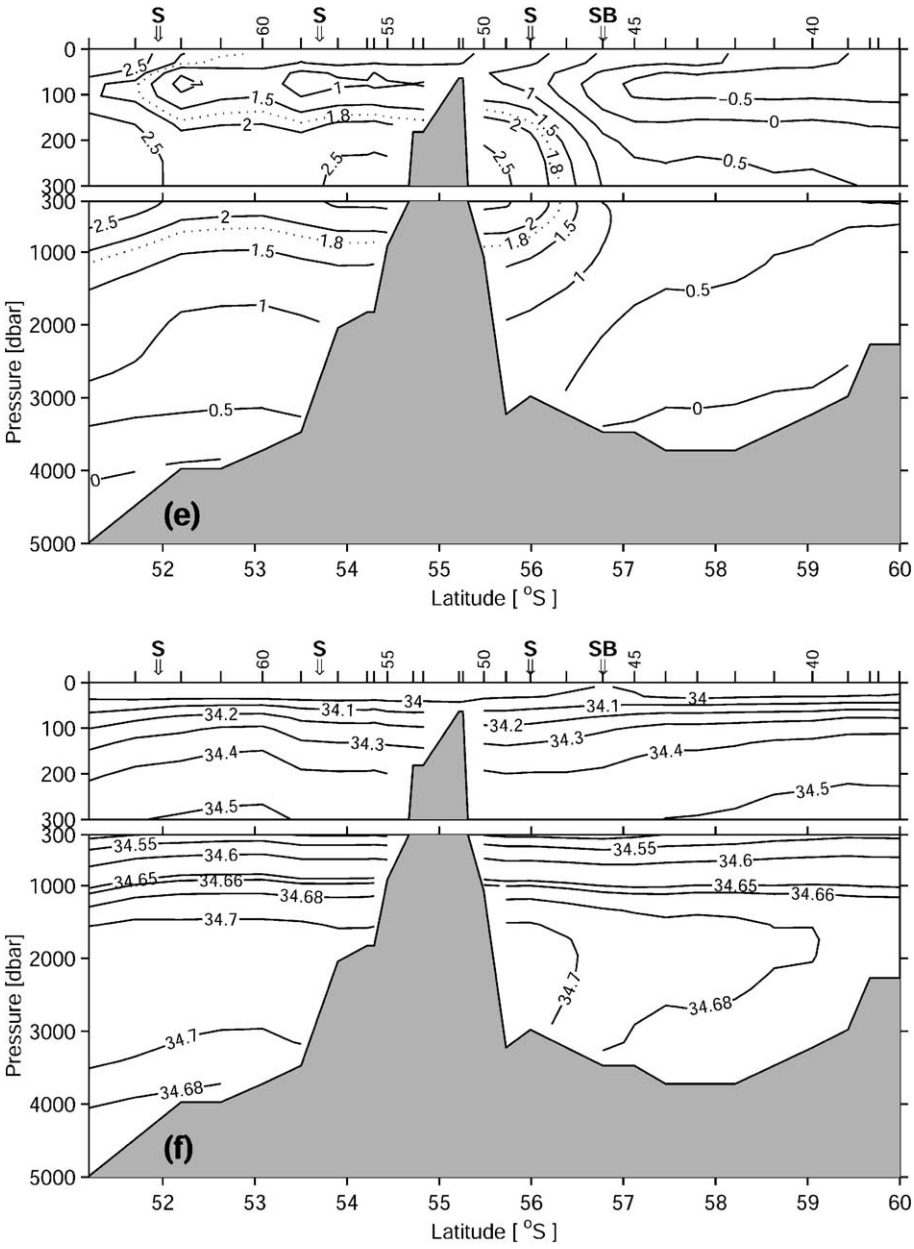

Fig. 3 (*continued*).

2.2. Mean position of the SACCF in historical hydrographic data

Potential temperature and salinity data were extracted from the World Ocean Database 1998, compiled by the Ocean Climate Laboratory of the National Oceanographic Data Center (Levitus et al., 1998). We incorporated an additional station that is absent from the dataset in its full depth form [station 281 (52.273°S, 41.747°W) from the RS *Melville* South Atlantic Ventilation Experiment (SAVE) cruise in 1989; downloaded from the Oceanographic Data

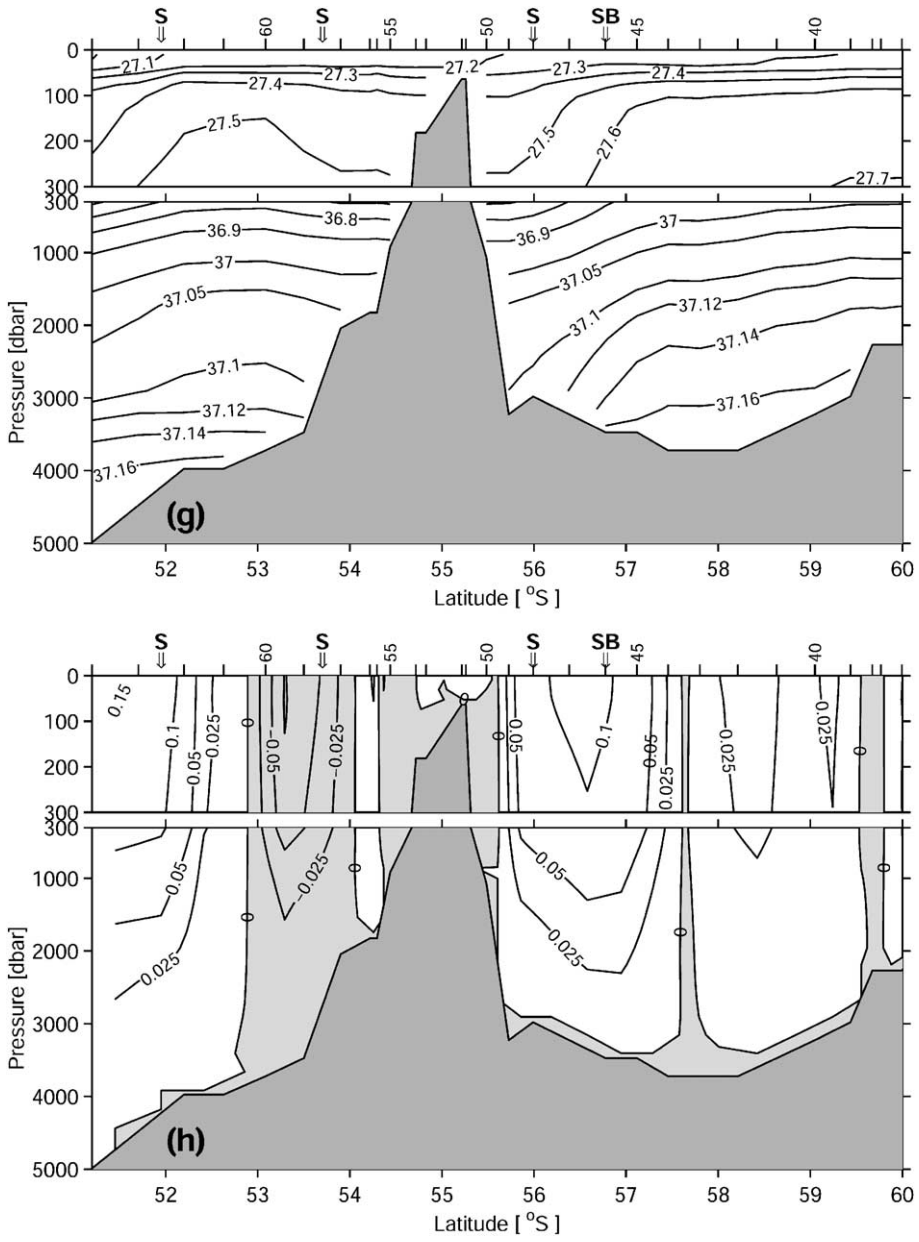

Fig. 3 (*continued*).

Server at Scripps Institute of Oceanography, http://nemo.ucsd.edu] but which appears to determine the western extent of the SACCF retroflection in the work of Orsi et al. (1995). After quality control, geopotential anomaly was calculated for 881 stations [Fig. 1(a)], covering the period of 1911–1990. We use 50 dbar as the upper reference level to remove possible seasonal variation in the data following Orsi et al. (1995). The lower reference level is set at 1000 dbar as many of the stations in the historical database do not have measurements to a depth greater than this; Gordon et al. (1978) show that this is a

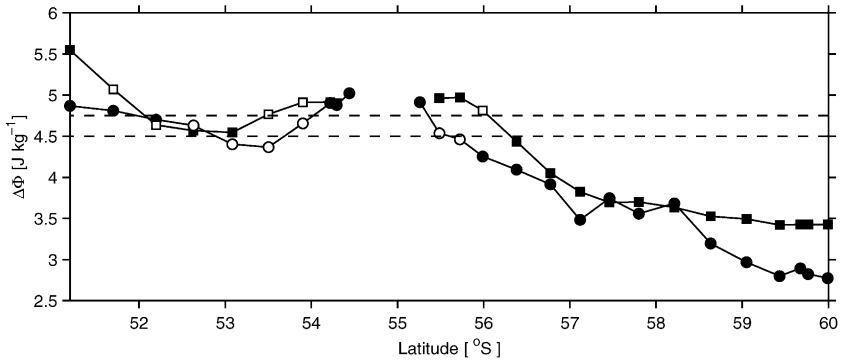

Fig. 4. Geopotential anomaly (50 dbar relative to 1000 dbar) along the A23 subsection (circles) and the OCCAM section (squares). Station pairs spanning the SACCF are marked in white. Dashed lines are at 4.5 and 4.75 J kg^{-1}.

suitable reference level for the surface flow of the Southern Ocean compared with a level of 3000 dbar. Before contouring, the historical geopotential anomaly field was gridded with a resolution of 1/4° × 1/4°, based on the spatial coverage of the data points [Fig. 1(a)].

The mean position of the SACCF in the geopotential anomaly field (as determined from the 4.5 J kg^{-1} contour; Fig. 5) shows that the front wraps around South Georgia, following the regional *f*/*h* contours which, because the variations in *f* are small over the study region, correspond to the bathymetry [Fig. 1(b)]. The increased number of stations available for the geopotential anomaly analysis as compared with those used by Orsi et al. (1995) [cf. Figs. 1(a) and 2] leads to significant differences in the mean positions of the SACCF. The SACCF is almost 100 km closer to the southern shelf of South Georgia than in the work of Orsi et al. (1995) and retroflects north of the island at approximately 36°W, 400 km east of the point of retroflection shown by Orsi et al. (1995) (Fig. 5). However, the closed contour rings in Fig. 5 are evidence for temporal variability associated with the SACCF representative of either shifts in the frontal position and/or the generation of eddies from the front. It is therefore possible, for example, that the SACCF does sometimes retroflect further west than our mean position shows (as shown in the following section), but we argue that the mean position of the SACCF resolved in our analysis is more representative. We now examine data from a near-surface drifter deployed in the South Georgia region as evidence for variability in the western extent of the SACCF retroflection.

2.3. Evidence from a near-surface drifter

Included in Fig. 5 is the trajectory of a near-surface drifter released as part of the WOCE/TOGA Surface Velocity Program in May 1996. The drifter (WMO ID 33568, released from 54.904°S, 39.898°W), drogued at 15 m depth, is the only drifter to become caught in the circulation around South Georgia demonstrating the retroflection of the flow north of the island. Released southwest of South Georgia, the drifter is advected onto the island's continental shelf and travels anticyclonically around the island before being deflected around the North Georgia Rise [cf. Fig. 1(b)] and into the faster-moving, deeper waters. Retroflection of the flow occurs near 41°W, providing evidence that the SACCF does at times extend beyond the mean position presented in Fig. 5. Because this is the only drifter trajectory available in this region, it can only provide information about the circulation at this one point in time. More drifters would help to elucidate the temporal variability associated with the flow.

The drifter has a mean speed of 0.17 m s^{-1}, faster than the geostrophic velocities derived for the SACCF from the A23 data. This implies that the resolution of the CTD stations was not high enough to accurately represent the frontal jet and/or that there is a significant barotropic component of the flow so that referencing to zero velocity at the deepest common level is not appropriate. The drifter provides evidence for anticyclonic eddies in the region north of South Georgia, becoming trapped in two. The first, in which the drifter spends 10 days, is encountered near the western flank of the North Georgia Rise. This recir-

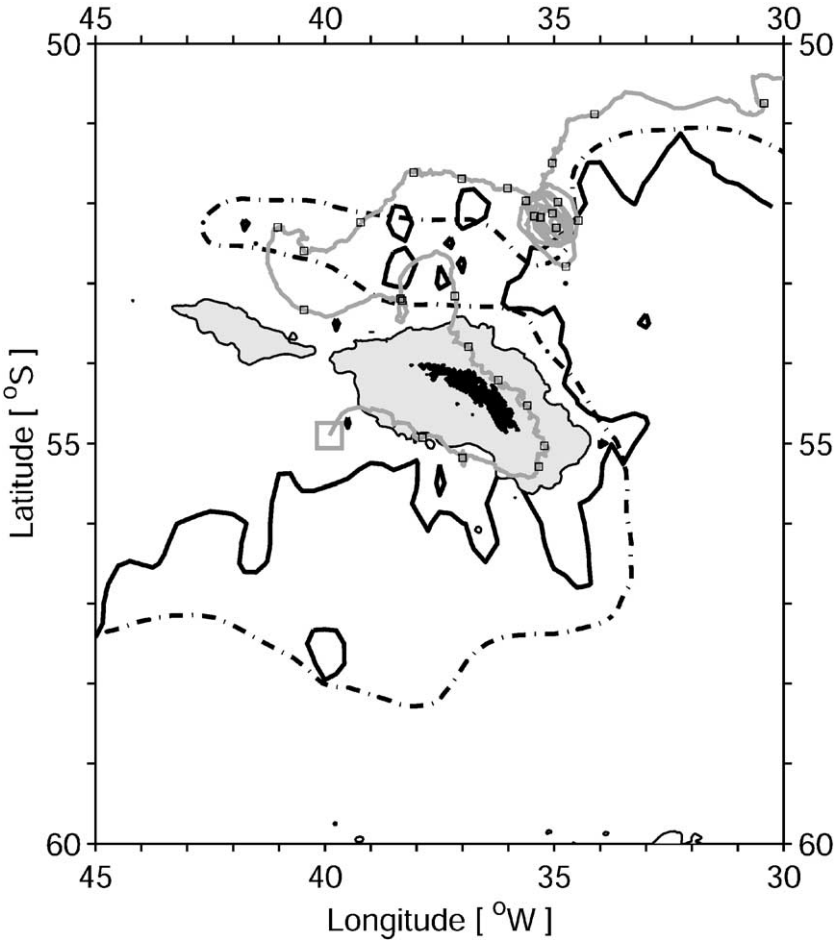

Fig. 5. Mean position of the SACCF from the historical geopotential anomaly analysis [solid black line; positions of the stations used in the analysis are marked in Fig. 1(a)] and from Orsi et al. (1995; dash-dotted black line). Areas shallower than 1000 m are shaded grey. Superimposed is the trajectory of a near-surface drifter (grey line) released in May 1996 from the position marked with a large square. Ten daily positions are marked with squares along the drifter's trajectory. The drifter data were obtained from the Marine Environmental Data Service: http://www.meds-sdmm.dfo-mpo.gc.ca.

culation has dimensions of $\sim 13 \times 33$ km; the local Rossby radius is $O(10$ km) (Houry et al., 1987). The second eddy, northeast of the North Georgia Rise, is much larger with a radius of approximately 45 km and detains the drifter for almost 3 months.

There are not sufficient hydrographic data available with which to investigate temporal variability associated with the SACCF retroflection. Instead we use output from a high resolution numerical global ocean circulation model forced with time variant fluxes to study the frontal behaviour.

3. The SACCF in OCCAM

3.1. OCCAM

Three years of potential temperature and salinity output from a high frequency wind forced run (1993–1995 inclusive) of the eddy-permitting Ocean Circulation and Climate Advanced Modelling project model (OCCAM) are used to calculate geopotential anomaly fields to locate the SACCF. OCCAM is a z level, high resolution ($1/4° \times 1/4°$ in the horizontal,

36 levels in the vertical, 20 m thick at the surface, 255 m thick at depth) primitive equation global ocean circulation model based on the Bryan–Cox–Semtner model but includes a free surface and improved advection schemes. Further details of the OCCAM formulation can be found in Webb et al. (1998) and Saunders et al. (1999). The model bathymetry was created from the US Navy DBDB5 topographic dataset with manual checking of the depth of key sills and channels (Thompson, 1995) and generally reproduces the main features of the regional bathymetry well [Fig. 1(b,c)]. Following 8 years of spin up with monthly mean winds, the wind forcing was changed to six hourly reanalysed winds from the European Centre for Medium-Range Weather Forecasts (ECMWF) with ECMWF sea level pressure applied at the model surface (Fox et al., 2000). Surface temperature and salinity were relaxed to monthly climatology (Levitus and Boyer, 1994; Levitus et al., 1994) with a time scale of 1 month. Five-day mean output fields are used in this analysis to remove the inertial oscillations that are a response to the high frequency forcing employed in the model (Jayne and Tokmakian, 1997).

3.2. The characteristics of the SACCF in OCCAM

Output from the high frequency wind forced run of OCCAM has been extracted along the Scotia Sea subsection of the WOCE A23 cruise to characterise the SACCF in the model. Potential temperature and salinity were bilinearly interpolated in space onto the station positions [Fig. 1(a)] from the two 5-day model fields spanning the occupation of the Scotia Sea leg.

As in the A23 subsection, the OCCAM section crosses the SACCF three times [near station 48, and between stations 58–59 and 62–63, e.g. Fig. 3(e)]. The northern and southern crossings of the front are slightly misplaced in OCCAM compared with the hydrographic data (by two stations in each case: $\sim$ 100 km at the northern and $\sim$ 55 km at the southern crossing). This could be due to the smoother bathymetry in the model, but it could also be a meander that is not predicted by the model.

There is a general northwards warming of the near-surface waters in the OCCAM A23 section [Fig. 3(e)], which means that the SACCF cannot reliably be detected in the θ_{min} properties as in the A23 data [Fig. 2(b)]. However, the front can be identified by characteristics of the UCDW: stations north of the SACCF have θ>2.5 °C at the θ-maximum [Figs. 2(b) and 3(e)]. The three SACCF crossings are associated with deep-reaching current cores [Fig. 3(h)]; the sense of the geostrophic velocities indicates that the front wraps anticyclonically around South Georgia in the model as in the hydrography. Maximum surface geostrophic velocities (relative to the deepest common level) in the SACCF in OCCAM are slightly faster than those in the hydrographic data: 0.15, $-$0.08 and 0.12 m s^{-1} for the crossings north to south, respectively. The southern jet is merged with that of the SB found two stations to the south of the SACCF (close to station 46). Baroclinic transport estimates are 23, 6 and 27 Sv, respectively, which for the northern and southern crossings of the front are much larger than the A23 values.

In accordance with the observation from the A23 and ALBATROSS data that the SACCF is associated with a consistent geopotential anomaly in this region, each crossing of the SACCF in the OCCAM section corresponds to a geopotential anomaly of 4.75 J kg^{-1} (Fig. 4). This is higher than the hydrographic value of 4.5 J kg^{-1} because the waters in the OCCAM section are almost 1 °C warmer than those in A23 [cf. Fig. 3(a,e)]. The geopotential anomaly signature is used in the following section to map the SACCF in each of the 5-day OCCAM fields to investigate temporal variability of the SACCF north of South Georgia.

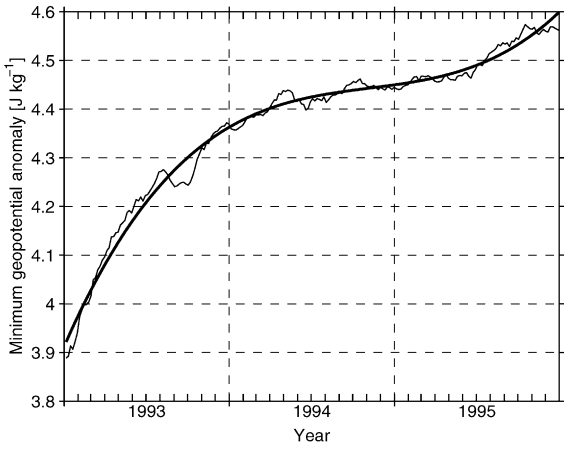

Fig. 6. Trend in minimum geopotential anomaly in OCCAM in the study region over the 3 years of model output (thin line). Thick line is the polynomial fit removed from the model geopotential anomaly. Tick marks represent the start of each month.

3.3. Variability in the western extent of the SACCF in OCCAM output

Saunders et al. (1999) show there to be a linear warming in the global potential temperature in the first run of OCCAM (forced with climatological wind stress from ECMWF). In the high frequency wind forced run of OCCAM, the drift continues but is nonlinear in the region around South Georgia. This introduces an increasing trend in the geopotential anomaly (Fig. 6). We correct for this by removing a third-order polynomial fit to the trend (Fig. 6) before contouring the geopotential anomaly field to locate the SACCF and investigate variability in the position of the front. This eliminates possible spurious effects during the 3-year run caused by using a changing geopotential anomaly to identify the SACCF.

The mean position of the SACCF in the South Georgia region in OCCAM, calculated by averaging all of the 5-day corrected geopotential anomaly fields during the 3-year period of model output, is shown in Fig. 7 overlaid on the mean velocity field from the model run at 52.35 m (level 3 in the model). The location of the front as defined by the geopotential anomaly corresponds to a jet in the velocity field. South and east of South Georgia, the jet is much

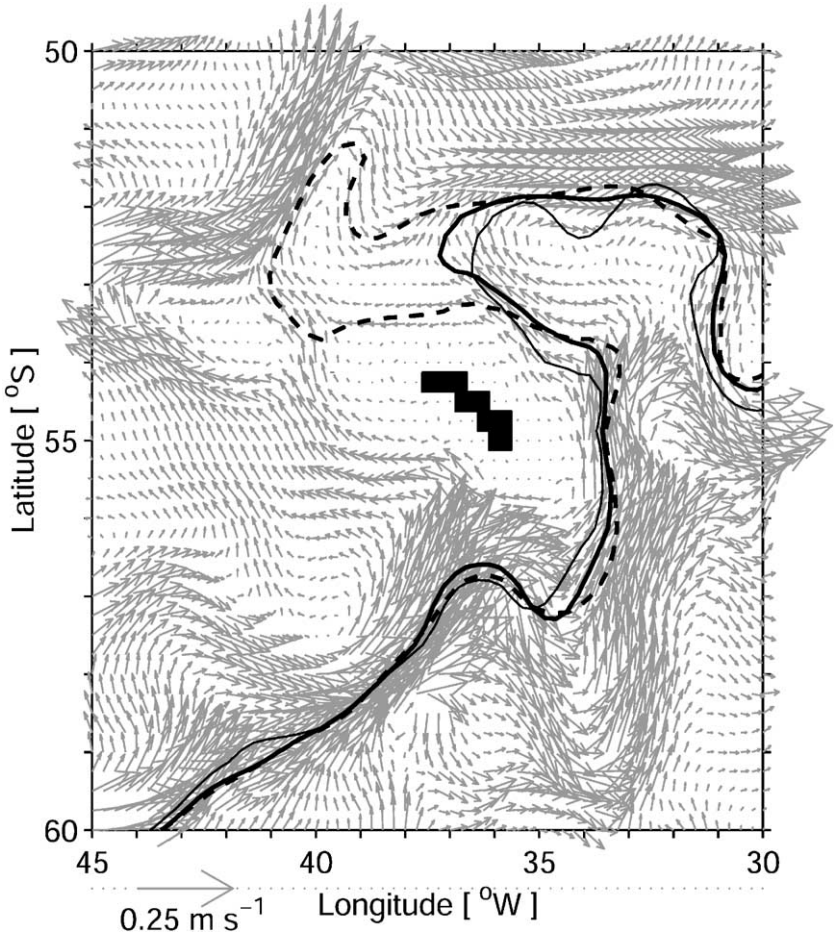

Fig. 7. Mean position and extrema of the SACCF in the high frequency wind forced run of OCCAM overlaid on the mean velocity field from the model run at 52.35 m (level 3 in the model). Thick solid line is the mean SACCF position over the 3 years of model output, and thin line is the position of the SACCF at its minimum western extent north of South Georgia (3 January 1993); thick dashed line is the position of the SACCF at its maximum western extent (29 December 1995).

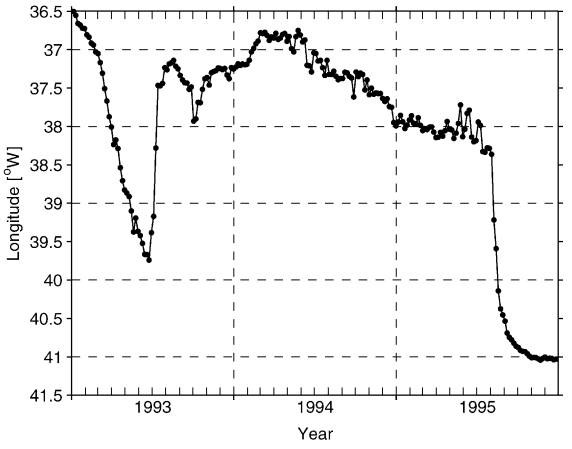

Fig. 8. Time series of the western extent of the SACCF retroflection north of South Georgia. Five-daily positions are marked with circles.

stronger than north of the island. East of South Georgia, the current splits; the main flow heads east and the remainder wraps anticyclonically around the island with the SACCF and a decreased velocity. The OCCAM A23 section showed that the jet associated with the southern crossing of the SACCF is merged with that of the SB; hence, the bifurcation of the current observed at $\sim 54°S$ may represent the separation of the SACCF and SB. Also visible in the velocity field is the Polar Front, which follows the southern flank of the Maurice Ewing Bank as reported from observations (Moore et al., 1997; Trathan et al., 1997, 2000).

North of South Georgia, the mean position of the SACCF in OCCAM is similar to that in the historical geopotential anomaly field (Fig. 5). South of South Georgia, however, the front is much further south of the island's shelf in the model due to anomalous water masses in the central Scotia Sea in OCCAM. These distort the regional flow and cause a southward deflection of the SACCF (Thorpe, 2001).

Analysis of the 5-day positions of the SACCF in OCCAM shows that the SACCF is not static north of South Georgia in the model but undergoes zonal movements. The range between the minimum and maximum western extent of the front in the model output is considerable, exceeding 300 km (Fig. 7). The maximum extent of the SACCF retroflection in the model is very close to the location of the front presented by Orsi et al. (1995) and is similar to the circulation illustrated by the drifter (Fig. 5). This suggests that the model represents the circulation of the ocean quite well north of South Georgia. The time

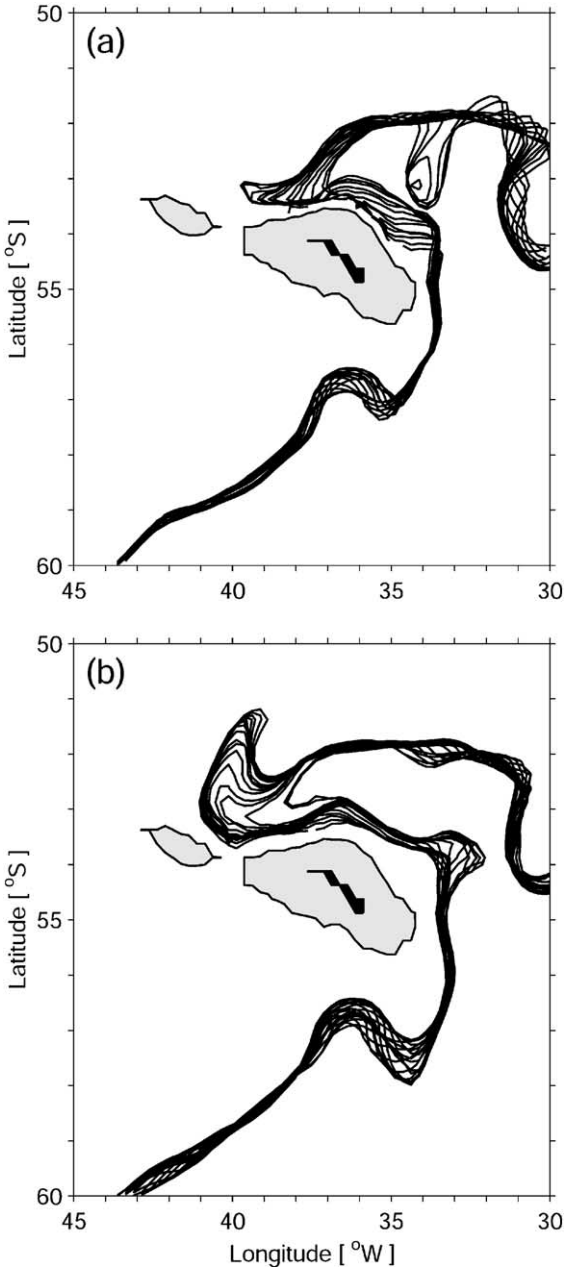

Fig. 9. Evolution of the two westward extensions of the SACCF north of South Georgia: (a) 1993; (b) 1995. Frontal positions, as determined from the model geopotential anomaly fields, are shown every 10 days. Areas shallower than 1000 m are shaded grey.

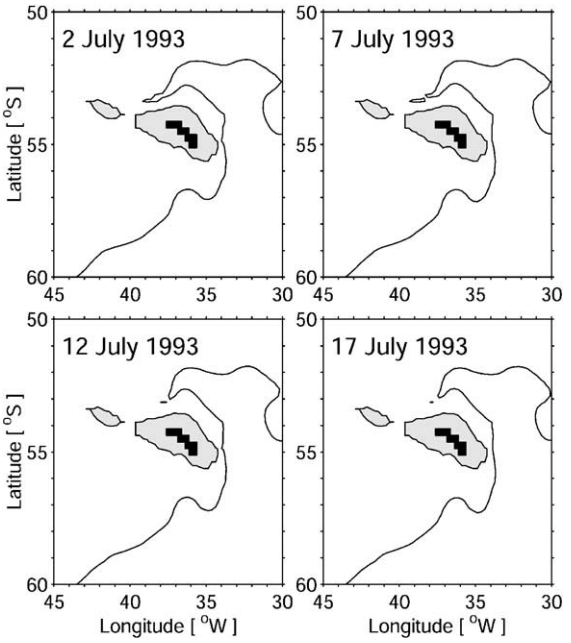

Fig. 10. The formation of an eddy from the SACCF retroflection in OCCAM. Each subplot shows the mean frontal position from a 5-day period starting at the date given. Areas shallower than 1000 m are shaded grey.

series of the frontal movements from the model is shown in Fig. 8. The SACCF extends west of South Georgia twice during the 3 years of model output, with maximum extent in June 1993 and December 1995. These westward extensions do not appear to be seasonal and vary in the time taken for the front to advance (95 days in 1993 cf. only 35 days in 1995 to move ~150 km). The shape of the SACCF as it extends differs between occasions (Fig. 9). In 1993, the SACCF is initially closer to the northern shelf of South Georgia than in 1995 and the point at which the front turns eastward along the island's northern shelf remains further west than in 1995. A cyclonic eddy is shed from the retroflection in 1993 and the SACCF retreats, whereas in 1995, the SACCF continues advancing until its path is blocked by the Polar Front, which deflects the SACCF northeastwards (Fig. 7).

Four consecutive snapshots of the SACCF show the formation of the eddy in 1993 (Fig. 10). Once the eddy is shed the front retreats rapidly, moving more than 130 km within 20 days. The eddy propagates eastwards and rejoins the SACCF a month later. The model run ends before we can see whether an eddy is shed at the end of the second westward shift in the retroflection. There is also evidence of warm core eddies forming along the SACCF with the same dimensions (radius of 45 km) as the large eddy visible in the drifter trajectory [Fig. 9(a)].

3.4. Implications for oceanic transport to South Georgia

Particles advected in the 5-day mean time-variant model velocity fields (52.35 m, level 3; Fig. 11) demonstrate the effect of the SACCF variability north

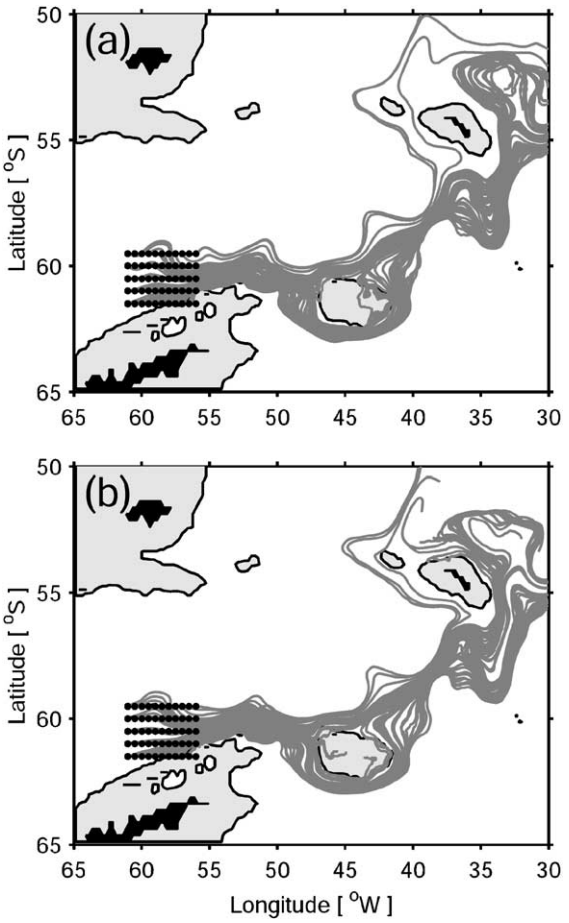

Fig. 11. Trajectories of particles tracked in the 5-day mean time-variant model velocity fields (52.35 m, level 3 in the model) released on (a) 1 January 1994 and (b) 1 January 1995. Release sites are marked with black circles. Areas shallower than 1000 m are shaded grey.

of South Georgia on transport into the region. Particles were released from the same sites close to the Antarctic Peninsula on 1 January 1994 and 1 January 1995, and tracked considering only advection with a second order Runge–Kutta scheme (Press et al., 1992). The problems with the model circulation in the southern Scotia Sea mentioned earlier mean that the particles follow a route along the South Scotia Ridge with many of the particles taken south of the South Orkney Plateau. The main difference in the particle trajectories occurs north of South Georgia. All of the particles released in 1994 remain north of the South Georgia shelf and have retroflected east of 37°W. Some of those released in 1995, however, reach the South Georgia shelf and are advected west of 40°W. The particles take about a year to cross the Scotia Sea and reach South Georgia. Referring back to Fig. 8, it can be seen that the particles that drift beyond South Georgia in 1995, arriving there towards the end of the year, correspond to a western extension of the SACCF. Similarly, the particles released in 1994 that reach South Georgia towards the end of 1994 but do not travel as far west as the later particles correspond to the SACCF being further east. Thus, if the SACCF is responsible for the advection of krill into the region north of South Georgia, the movements in the front will contribute to the variability observed in the South Georgia ecosystem.

Particles were also released into the model velocity fields, calculated for 15 m depth by weighting the upper two levels of the model, at the point of deployment of the drifter discussed in Section 2.3. However, the particles do not behave like the drifter and are taken northwards between South Georgia and Shag Rocks [marked in Fig. 1(b)] or west around Shag Rocks and northwards, similar to the tracks shown in Fig. 11 that pass close to Shag Rocks. This is due to a too strong Ekman effect in the model.

4. Discussion

The use of geopotential anomaly to locate the SACCF allows all available historical data to be used in this analysis (subject to quality control), including data that are not part of a synoptic section. This has given high horizontal resolution (1/4° × 1/4°) of the circulation features in the eastern Scotia Sea. The mean large-scale circulation as illustrated by the geopotential anomaly field agrees with the work of Gordon et al. (1978), Olbers et al. (1992) and Orsi et al. (1995), who all use historical datasets to show water from the southern ACC wrapping around South Georgia. Only Orsi et al. (1995) have resolved the position of the SACCF in the study region; our analysis shows the mean position of the retroflection of the SACCF to be at about 36°W, approximately 6° east of the corresponding position in the work of Orsi et al. (1995), and the front to be much closer to the southern shelf of South Georgia.

Mesoscale variability in the region north of South Georgia is evident in the geopotential anomaly field and in the drifter trajectory. OCCAM demonstrates both zonal movement of the front and eddy-shedding from the retroflection north of South Georgia. Trathan et al. (1997) describe variability in the physical oceanographic characteristics in the region northwest of South Georgia that suggests large-scale changes in the position of the SACCF on monthly time scales. This is consistent with the OCCAM results: between January and February 1994 (corresponding to the observation period of Trathan et al., 1997), the SACCF moves eastward by 30 km in the model.

The generation of eddies from the SACCF is important for cross-frontal transfer of properties into the waters north of the SACCF. The waters south of the SACCF, influenced by the Weddell–Scotia Confluence, are rich in nutrients, especially silicate; hence, eddies from the SACCF could be an important mechanism for the enhancement of local productivity (Whitehouse et al., 1996). The cold core eddy that was formed in OCCAM rejoined the SACCF after 1 month; data from the Southern Ocean Argo program (a global array of temperature/salinity profiling floats; Roemmich and Owens, 2000) should help to describe the characteristics and fate of these eddies in the ocean.

The variability observed in the hydrographic data and model output of the SACCF north of South Georgia is likely to be significant for the marine predator populations breeding on the western end of South Georgia. The breeding success of the predators is linked to the local abundance of krill. If, as hypothesised, the SACCF and the waters south of it are responsible for the transport of krill into the region, times when the front is further east could

mean reduced availability of krill for the predators. Our analysis of historical hydrographic data has shown the mean position of the SACCF to be much further east than in other work; this makes fluctuations in the western extent of the front much more important in terms of delivering krill into regions accessible by the predators. Eddies shed from the front may also transport krill into the region, thus the timing and frequency of these events and the fate of the eddies may have an impact on the South Georgia ecosystem. The resolution of the close proximity of the SACCF to the southern shelf of South Georgia shows that the SACCF may play an important role in transport to the southern South Georgia region. Once material reaches the South Georgia shelf, on-shelf processes such as tides may act to retain or circulate it on-shelf. These processes could provide an alternative transport route for passive drifters to reach the western end of South Georgia.

Finally, a note on the dynamics of the system. The short period of model output, with only two occurrences of the large westward shift in the position of the retroflection, means that we cannot definitively determine the mechanisms for the westward extensions of the SACCF and the related eddy-shedding. However, the wind forcing in the run of OCCAM considered here is the only forcing that is not cyclical (recall that surface temperature and salinity are relaxed to monthly climatological Levitus 1994 data, Section 3.1). The infrequency of the large extensions of the SACCF retroflection suggests that there might be a signal in the wind stress that predisposes the front to move zonally. Time series of the mean zonal and meridional wind stress averaged over the Scotia Sea (50–65°S, 70–30°W) and over the study region, however, show no consistent feature that corresponds to the westward extensions of the SACCF. This suggests that wind stress does not play a direct role in triggering the movements of the front. To strengthen this conclusion, mean annual output from the first run of OCCAM that was forced with cyclical climatological monthly wind fields (Webb et al., 1998; Saunders et al., 1999) has been examined. The repetitive wind forcing means that if the movements of the SACCF north of South Georgia were due to wind forcing, the mean annual positions of the front should be similar since the frontal extensions should occur at approximately the same time and rate each year. However, they are not, suggesting that the extensions of the SACCF are the result of inherent instability in the modelled current rather than being a wind forced feature. We investigated possible relationships between the frontal movements and variations in the volume transport of the SACCF and the ACC but found no direct link.

The SACCF north of South Georgia, with its westward extensions and evidence for subsequent eddy shedding, appears similar to the Agulhas Current south of Africa. Both currents are western boundary currents and both follow f/h contours. The Agulhas Current is significantly more active than the SACCF (shedding much larger eddies at an approximate rate of six per year; De Ruijter et al., 1999) but it is associated with a much larger transport (73 Sv; Beal and Bryden, 1999). Pichevin et al. (1999) assert that the Agulhas Current sheds eddies to balance the zonal momentum flux associated with the retroflecting current. As the transport of the SACCF is much smaller than that of the Agulhas Current, it is likely that the SACCF would not need to shed eddies as frequently as the Agulhas Current, nor would the rings need to be as large. This is what we observe in the OCCAM output. However, the association between the SACCF and the Agulhas Current is speculation at this stage and it is possible that the dynamics governing the two systems are completely different. A longer time series of model output and more detailed studies, such as process models, are required to better understand the dynamics of the SACCF in this region.

5. Summary

Analysis of historical hydrographic data in the South Georgia region of the Southern Ocean has mapped the SACCF at high resolution. The front follows the local bathymetry, wrapping anticyclonically around South Georgia and retroflecting north of the island at ~36°W, 400 km east of the published mean position of the front. The geopotential anomaly field revealed temporal variability associated with the position of the SACCF north of South Georgia, suggesting shifts in the frontal position and/or the formation of eddies from the SACCF. Both processes are likely to be important for the local marine ecosystem by affecting the influx of krill into the region.

The trajectory of a near-surface drifter released southwest of South Georgia showed that the SACCF can extend much further west than the mean position.

A realistically forced global ocean circulation model (OCCAM) showed the SACCF to be dynamic in the region north of South Georgia with large zonal extensions covering a range of 300 km and shedding of both cyclonic and anticyclonic eddies. Trajectories of particles tracked in the time-variant model velocity fields demonstrate that the frontal movements do affect transport into the South Georgia region and are therefore likely to be of importance to the South Georgia ecosystem. It is possible that the SACCF variability results from inherent instability of the modelled current rather than direct wind forcing, but further research into the system is required to determine the frontal dynamics.

Acknowledgements

We thank Andrew Coward and Beverly de Cuevas for their help extracting the OCCAM output and wind data. We had useful discussions with David Webb about OCCAM and Keith Reid about krill dynamics in the South Georgia ecosystem. We are grateful to Igor Belkin and two anonymous reviewers for their constructive comments that helped to much improve the manuscript. WOCE section A23 was funded by the Natural Environment Research Council (NERC) through grant GST/02/575. This research was funded by a NERC CASE PhD studentship between the University of East Anglia and the British Antarctic Survey.

References

Atkinson, A., Whitehouse, M.J., Priddle, J., Cripps, G.C., Ward, P., Brandon, M.A., 2001. South Georgia, Antarctica: a productive, cold water, pelagic ecosystem. Mar. Ecol. Prog. Ser. 216, 279–308.

Beal, L.M., Bryden, H.L., 1999. The velocity and vorticity structure of the Agulhas Current at 32°S. J. Geophys. Res. 104, 5151–5176.

Boyd, I.L., Arnould, J.P.Y., Barton, T., Croxall, J.P., 1994. Foraging behaviour of Antarctic fur seals during periods of contrasting prey abundance. J. Anim. Ecol. 63, 703–713.

Brandon, M.A., Murphy, E.J., Whitehouse, M.J., Trathan, P.N., Murray, A.W.A., Bone, D.G., Priddle, J., 1999. The shelf break front to the east of the sub-Antarctic island of South Georgia. Cont. Shelf Res. 19, 799–819.

Brandon, M.A., Murphy, E.J., Trathan, P.N., Bone, D.G., 2000. Physical oceanographic conditions to the northwest of the sub-Antarctic island of South Georgia. J. Geophys. Res. 105, 23983–23996.

Croxall, J.P., McCann, T.S., Prince, P.A., Rothery, P., 1988. Reproductive performance of seabirds and seals at South Georgia and Signy Island, South Orkney Islands, 1976–1987: implications for Southern Ocean monitoring studies. In: Sahrhage, D. (Ed.), Antarctic Ocean and Resources Variability. Springer-Verlag, Berlin, pp. 261–285.

Croxall, J.P., Reid, K., Prince, P., 1999. Diet, provisioning and productivity responses of predators to differences in availability of Antarctic krill. Mar. Ecol. Prog. Ser. 177, 115–131.

Deacon, G.E.R., 1933. A general account of the hydrography of the South Atlantic Ocean. Discov. Rep. 7, 171–238.

Deacon, G.E.R., 1977. Seasonal and annual variations in water temperature and salinity near South Georgia 1925–1937. Report No. 49, Institute of Oceanographic Sciences, Wormley, UK.

De Ruijter, W.P.M., Biastoch, A., Drijfhout, S.S., Lutjeharms, J.R.E., Matano, R.P., Pichevin, T., van Leeuwen, P.J., Weijer, W., 1999. Indian–Atlantic interocean exchange: dynamics, estimation and impact. J. Geophys. Res. 104, 20885–20910.

Everson, I., 1977. The living resources of the Southern Ocean. GLO/SO/77/1. Food and Agricultural Organization, Rome. 156 pp.

Everson, I., 1984. Marine interactions. In: Laws, R.M. (Ed.), Antarctic Ecology, vol. 2. Academic Press, London, pp. 783–819.

Fox, A.D., Haines, K., de Cuevas, B.A., Webb, D.J., 2000. Altimeter assimilation in the OCCAM global model: Part II. TOPEX/POSEIDON and ERS-1 assimilation. J. Mar. Syst. 26, 323–347.

Gordon, A.L., 1967. Structure of Antarctic waters between 20°W and 170°W. In: Bushnell, V.C. (Ed.), Antarctic Map Folio Ser. No. 6. Am. Geophys. Soc., New York. 10 pp.

Gordon, A.L., Molinelli, E., Baker, T., 1978. Large-scale relative dynamic topography of the Southern Ocean. J. Geophys. Res. 83, 3023–3032.

Harmer, S.F., 1931. Southern whaling. Proc. Linn. Soc. Lond. 142, 85–163.

Heywood, K.J., King, B.A., 1996. WOCE Section A23 Cruise Report. UEA Cruise Rep. Series 1. School of Environmental Sciences, University of East Anglia, Norwich, UK.

Heywood, K.J., Sparrow, M.D., Brown, J., Dickson, R.R., 1999. Frontal structure and Antarctic bottom water flow through the Princess Elizabeth Trough, Antarctica. Deep-Sea Res., Part I 46, 1181–1200.

Hofmann, E.E., Klinck, J.M., Locarnini, R.A., Fach, B., Murphy, E., 1998. Krill transport in the Scotia Sea and environs. Antarct. Sci. 10, 406–415.

Houry, S., Dombrowsky, E., de Mey, P., Minster, J.-F., 1987. Brunt–Väisälä frequency and Rossby radii in the South Atlantic. J. Phys. Oceanogr. 17, 1619–1626.

Jayne, S.R., Tokmakian, R., 1997. Forcing and sampling of ocean general circulation models: impact of high-frequency motions. J. Phys. Oceanogr. 27, 1173–1176.

Levitus, S., Boyer, T.P., 1994. World Ocean Atlas 1994. Vol. 4:

Temperature. NOAA Atlas NESDIS 4. U.S. Gov. Printing Off., Washington, DC. 117 pp.

Levitus, S., Burgett, R., Boyer, T.P., 1994. World Ocean Atlas 1994. Vol. 3: Salinity. NOAA Atlas NESDIS 3. U.S. Gov. Printing Off., Washington, DC. 111 pp.

Levitus, S., Boyer, T.P., Conkright, M.E., O'Brien, T., Antonov, J., Stephens, C., Stathoplos, L., Johnson, D., Gelfeld, R., 1998. World Ocean Database 1998. Vol. 1: Introduction. NOAA Atlas NESDIS 18. U.S. Gov. Printing Off., Washington, DC. 346 pp.

Loeb, V., Siegel, V., Holm-Hansen, O., Hewitt, R., Fraser, W., Trivelpiece, W., Trivelpiece, S., 1997. Effects of sea-ice extent and krill or salp dominance on the Antarctic food web. Nature 387, 897–900.

Marr, J.W.S., 1962. The natural history and geography of the Antarctic krill (*Euphausia superba* Dana). Discov. Rep. 32, 33–64.

Maslennikov, V.V., Solyankin, E.V., 1979. Inter-annual shift of zones where the waters of the Weddell Sea and the Antarctic Circumpolar Current interact. Antarctica, vol. 18. Nauka, Moscow, pp. 118–122.

Meredith, M.P., Naveira Garabato, A.C., Stevens, D.P., Heywood, K.J., Sanders, R.J., 2001. Deep and bottom waters in the eastern Scotia Sea: rapid changes in properties and circulation. J. Phys. Oceanogr. 31, 2157–2168.

Moore, J.K., Abbott, M.R., Richman, J.G., 1997. Variability in the location of the Antarctic Polar Front (90°–20°W) from satellite sea surface temperature data. J. Geophys. Res. 102, 27825–27833.

Murphy, E.J., Watkins, J.L., Reid, K., Trathan, P.N., Everson, I., Croxall, J.P., Priddle, J., Brandon, M.A., Brierley, A.S., Hofmann, E., 1998. Interannual variability of the South Georgia marine ecosystem: biological and physical sources of variation in the abundance of krill. Fish. Oceanogr. 7, 381–390.

Olbers, D., Gouretski, V., Seiß, G., Schröter, J., 1992. Hydrographic Atlas of the Southern Ocean Alfred Wegener Institute, Bremerhaven. 82 pp., 82 plates.

Orsi, A.H., Whitworth III, T., Nowlin Jr., W.D., 1995. On the meridional extent and fronts of the Antarctic Circumpolar Current. Deep-Sea Res., Part 1 42, 641–673.

Park, Y.-H., Charriaud, E., Craneguy, P., Kartavtseff, A., 2001. Fronts, transport and Weddell Gyre at 30°E between Africa and Antarctica. J. Geophys. Res. 106, 2857–2879.

Pichevin, T., Nof, D., Lutjeharms, J., 1999. Why are there Agulhas Rings? J. Phys. Oceanogr. 29, 693–707.

Press, W.H., Teukolsky, S.A., Vetterling, W.T., Flannery, B.P., 1992. Numerical Recipes in FORTRAN, 2nd ed. Cambridge Univ. Press, Cambridge, UK, 963 pp.

Reid, K., Barlow, K.E., Croxall, J.P., Taylor, R.I., 1999a. Predicting changes in the Antarctic krill, *Euphausia superba*, population at South Georgia. Mar. Biol. 135, 647–652.

Reid, K., Watkins, J.L., Croxall, J.P., Murphy, E.J., 1999b. Krill population dynamics at South Georgia 1991–1997, based on data from predators and nets. Mar. Ecol. Prog. Ser. 177, 103–114.

Rintoul, S.R., Bullister, J.L., 1999. A late winter hydrographic section from Tasmania to Antarctica. Deep-Sea Res., Part 1 46, 1417–1454.

Rintoul, S.R., Sokolov, S., 2001. Baroclinic transport variability of the Antarctic Circumpolar Current south of Australia (WOCE repeat section SR3). J. Geophys. Res. 106, 2815–2832.

Roemmich, D., Owens, W.B., 2000. The Argo Project: global ocean observations for understanding and prediction of climate variability. Oceanography 13, 45–50.

Saunders, P.M., Coward, A.C., de Cuevas, B.A., 1999. Circulation of the Pacific Ocean seen in a global ocean model: Ocean Circulation and Climate Advanced Modelling project (OCCAM). J. Geophys. Res. 104, 18281–18299.

Siegel, V., Loeb, V., 1995. Recruitment of Antarctic krill *Euphausia superba* and possible causes for its variability. Mar. Ecol. Prog. Ser. 123, 45–56.

Siegel, V., Loeb, V., Gröger, J., 1998. Krill (*Euphausia superba*) density, proportional and absolute recruitment and biomass in the Elephant Island region (Antarctic Peninsula) during the period 1977 to 1997. Polar Biol. 19, 393–398.

Smith, W.F., Sandwell, D.T., 1997. Global seafloor topography from satellite altimetry and ship depth soundings. Science 277, 1956–1962.

Sparrow, M.D., Heywood, K.J., Brown, J., Stevens, D.P., 1996. Current structure of the south Indian Ocean. J. Geophys. Res. 101, 6377–6391.

Thompson, S.R., 1995. Sills of the global ocean: a compilation. Ocean Model. 109, 7–9.

Thorpe, S.E., 2001. Variability of the southern Antarctic Circumpolar Current in the Scotia Sea and its implications for transport to South Georgia. PhD thesis, University of East Anglia, Norwich, UK, 212 pp.

Trathan, P.N., Brandon, M.A., Murphy, E.J., 1997. Characterization of the Antarctic Polar Frontal Zone to the north of South Georgia in summer 1994. J. Geophys. Res. 102, 10483–10497.

Trathan, P.N., Brandon, M.A., Murphy, E.J., Thorpe, S.E., 2000. Transport and structure within the Antarctic Circumpolar Current to the north of South Georgia. Geophys. Res. Lett. 27, 1727–1730.

Veth, C., Peeken, I., Sharek, R., 1997. Physical anatomy of fronts and surface waters in the ACC near the 6°W meridian during austral spring 1992. Deep-Sea Res., Part 2 44, 23–49.

Webb, D.J., de Cuevas, B.A., Coward, A.C., 1998. The first main run of the OCCAM global ocean model. Internal Document 34, Southampton Oceanography Centre.

Whitehouse, M.J., Priddle, J., Trathan, P.N., Brandon, M.A., 1996. Substantial open-ocean phytoplankton blooms to the north of South Georgia, South Atlantic, during summer 1994. Mar. Ecol. Prog. Ser. 140, 187–197.

Whitworth III, T., Nowlin Jr., W.D., Orsi, A.H., Locarnini, R.A., Smith, S.G., 1994. Weddell Sea shelf water in the Bransfield Strait and Weddell–Scotia Confluence. Deep-Sea Res., Part 1 41, 629–641.